How Well Does Microsolvation Represent Macrosolvation? A Test Case: Dynamics of Decarboxylation of 4-Pyridylacetic Acid Zwitterion

Daria Sicinska,[†] **Piotr Paneth,***[,†] **and Donald G. Truhlar***[,‡]

Institute of Radiation Chemistry, Technical University of Lodz, Zeromskiego 116, 90−924 Lodz, Poland, and Department of Chemistry and Supercomputing Institute, University of Minnesota, Minneapolis, Minnesota 55455-0431

We present a systematic comparison of a cluster model to a continuum solvation model for the rate of decarboxylation of 4-pyridylacetic acid zwitterion. Geometries of the zwitterion and the transition state were optimized for the gas-phase reaction, for one model of reaction in aqueous solution in a previous study, and for five additional models of reaction in aqueous solution in the present study. The aqueous calculations include models in which one or two waters are treated explicitly, either without or with a surrounding continuum of bulk solvent; the latter is called a mixed discrete-continuum model. Bulk solvation effects are modeled both by solvation model SM5.42 and by a COSMO united atom solvation model; both of these models contain bulk electrostatics and short-range terms. Kinetic isotope effects were calculated by conventional transition state theory. We find that a discrete model of solvation with two explicit water molecules underestimates the free energy of activation for the decarboxylation reaction by at least 17 kcal/mol.

1. Introduction

Experimental and theoretical techniques for studying clusters continue to yield new insights into a variety of finite-size systems. Clusters are important in their own right and also as components of nanomaterials. However, another aspect of clusters that continues to intrigue us is the question: how well does microsolvation in a cluster mimic solvation by a bulk liquid? This question has been widely studied,[1] along with a closely related one: when bulk solvation is modeled by surrounding the solute with a continuum solvent model are the results improved by making one or a few solvent molecules explicit and then surrounding the solute/explicit-solvent cluster with a continuum? (This is sometimes called a mixed discrete-continuum solvation model.)

When specific solute−solvent interactions are important, e.g., an acid−base reaction in water or any reaction involving charge separation and hydrogen bonding, one might consider whether the supermolecule approach (in which a few solvent molecules noncovalently bound to the solute are added explicitly to the solute to form a solute−solvent supersystem or supermolecule) is to be preferred to treating solvent as a continuum.[2] Or one could treat a few solvent molecules explicitly and still use bulk solvation models for the rest.[3] However, the addition of explicit solvent molecules, with or without further solvent treated as a continuum, has its own problems. First of all, the quantitative calculation of the strength of individual solute−solvent interactions is a difficult problem in its own right. Second, it is not clear how to determine the number and orientation of nonbulk solvent molecules. In many cases a complete first solvation shell of even a medium-sized solute involves hundreds of orientations that constitute local minima. The only satisfactory way to average over these orientations is to perform a full Monte Carlo

or molecular dynamics simulation involving explicit waters in at least the second solvation shell as well. In such simulations, one typically[4] (but not always[5]) treats the solute as rigid and nonpolarizable. Polarizable explicit solvent models are under development,[6] but at the present time, it is unclear whether these deficiencies can be overcome realistically and efficiently enough for simulations with full explicit solvent to be reliable, and the supermolecule approach with only a few waters is even more questionable. Nevertheless, each of these models may be the preferred compromise of efficiency and expected reliability for particular problems under particular circumstances. Therefore, it is important to compare their predictions for prototype systems. A particularly interesting prototype to be studied is the case of decarboxylation reactions because we have recently pointed out that decarboxylation reactions provide a very clear example of solvent-dependent transition states, apparently the most definitive example of this phenomenon ever observed.[7] Therefore, it is of great interest to understand these solvent effects from a fundamental point of view, and so we chose them for a systematic examination of the two questions posed in the first paragraph. We report here the comparison of discrete, continuum, and mixed discrete/continuum models for the rate of decarboxylation of 4-pyridylacetic acid in water.

2. Calculations

Our liquid-phase calculations are based on the Hartree−Fock (HF) method[8] with the 6-31G(d) basis set[9] and the SM5.42 solvation model.[10] To avoid possible confusion, we note at the outset that we directly calculate free energy changes in solution; we do *not* proceed by adding changes in the free energy of solvation to changes in gas-phase energies (in fact our results are independent of gas-phase geometries, and we did not calculate free energies of solvation, which are irrelevant in our direct procedure). The SM5.42 model includes geometry optimization in the presence of the solvent, which is represented by a continuum model with bulk electrostatic effects[11] treated

* To whom correspondence should be addressed.
† Technical University of Lodz.
‡ University of Minnesota.

self-consistently with solute polarization[11d,11g] and first-solva-tion-shell effects treated in terms of atomic solvent-accessible surface areas[12] (SASAs). The bulk electrostatic terms are calculated by the generalized Born (GB) approximation[11] for a continuum dielectric representation of the solvent. The electrostatic term represents a statistical average over the electric polarization effects in an ensemble of solvent configurations, and it includes both electronic and nuclear polarization of the solvent and solute. The first-solvation-shell terms are based on empirical atomic surface tensions that model the difference between the true solvation free energy and that calculated by the bulk electrostatic term.[10,11g] When the electrostatic term is based on a realistic representation of the solute charge distribution, as it is in the SM5.42 model, then this difference is dominated by the first solvation shell, especially by cavitation, dispersion, and solvent-structure effects. The atomic surface tensions are multiplied by atomic SASAs that are continuous functions solute geometry; the continuous SASAs are assumed to represent a statistical average over a variable number of discrete solvent molecules in the first solvation shell.

The solute is 4-pyridylacetic acid, and the solvent is water, which may be explicit, implicit, or mixed. Let ψ_g and ψ_l denote gas-phase and liquid-phase electronic wave functions for the explicit systems, i.e., for the solute and (if present) explicit solvent, and let R_g and R_l denote gas-phase and liquid-phase geometries for the explicit system. Note that ψ_l and R_l are determined in the presence of continuum solvent, whereas for ψ_g and R_g, the explicit system is isolated from the bulk solvent. Let $\mathscr{H}_0$ be the gas-phase electronic Hamiltonian (including nuclear repulsion) of the explicit system, and let θ denote the additional terms (electrostatic and atomic-surface-tension terms) that generate the free energy of the explicit system in a liquid-phase environment. We consider four approximations to the free energy of the liquid-phase species.

1. Continuum Solvent. In this case, the free energy of the liquid is written

$$G(l) = \mathscr{H}_0(\psi_g, R_g) + \Delta G_S + E_0(g|vib) + \Delta G_{298}(g|vibrot) \quad (1)$$

where $E_0(g|vib)$ is the gas-phase zero-point energy, $\Delta G_{298}(g|vibrot)$ is the difference between the vibrational−rotational free energy at 298 K and its value (which equals the zero point energy) at 0 K, and ΔG_S is the free energy of solvation. The latter is given by

$$\Delta G_S = \mathscr{H}_0(\psi_l, R_l) + \theta(\psi_l, R_l) - \mathscr{H}_0(\psi_g, R_g) \quad (2)$$

Combining (1) and (2) and adding and subtracting $\mathscr{H}_0(\psi_g, R_l)$ allows us to write

$$G(l) = \mathscr{H}_0(\psi_g, R_l) + \Delta\mathscr{H}(R_l) + \theta(\psi_l, R_l) + E_0(g|vib) + \Delta G_{298}(g|vibrot) \quad (3)$$

where

$$\Delta\mathscr{H}(R_l) = \mathscr{H}_0(\psi_l, R_l) - \mathscr{H}_0(\psi_g, R_l) \quad (4)$$

We use the SM5.42/HF/6-31G(d) model to optimize R_l and to calculate $\Delta\mathscr{H}(R_l)$ and $\theta(\psi_l, R_l)$. However, the first term of eq 3 is evaluated at a higher level, namely, the correlated multicoefficient quadratic configuration interaction with single and double excitations[13] (MC-QCISD) method. (The other terms of eq 3 are not affected by the MC-QCISD correction.) This combination is denoted MC-QCISD + SM5.42/HF/6-31G(d)//

SM5.42/HF/6-31G(d), or, for short, as SM5.42. Notice that all calculations are performed at R_l; the gas-phase geometry is totally irrelevant to evaluating free energies in the liquid phase, except for its use in the last two terms of eq 1, although it would of course be needed for evaluating free energies of solvation, which are not used here.

2. Mixed Discrete/Continuum Model. This model is the same as above except that one or two explicit solvent molecules are added to the solute to constitute the explicit system. The geometry R_l is reoptimized for this extended system in the presence of the continuum liquid. These calculations are denoted discrete(n) + SM5.42, where n is the number of explicit solvent molecules. We did introduce a further approximation though in that the first term of eq 3 was approximated by HF/6-31G(d)//SM5.42/HF/6-31G(d) for one or two explicit solvent molecules plus the same MC-QCISD correction (−2.6 kcal/mol) that was calculated with no explicit solvent.

3. Discrete Model. In this model, the terms ΔG_S and θ are omitted, but the explicit system contains one or two solvent molecules plus the solute. The geometry R_l is reoptimized for this extended system in the absence of continuum liquid. These calculations are denoted discrete(n) where n is 1 or 2. The electronic energy E is obtained as the sum of the HF/6-31G(d) energy for $n = 1$ or 2 and the same MC-QCISD correction (−2.6 kcal/mol) as used above.

4. Gas-Phase. In this model, the explicit system is simply the solute, and $\Delta G_S = 0$. The gas-phase solute geometry is used. The electronic energy E is obtained as the sum of the HF/6-31G(d) energy for $n = 0$ plus the same MC-QCISD correction as used above.

For the discrete and gas-phase cases, one can also obtain the 298 K enthalpy $H_{298}^\ddagger$ or H_{298}^R instead of $G_{298}^\ddagger$ or G_{298}^R by replacing the $\Delta G_{298}(g|vibrot)$ term by $\Delta H_{298}(g|vibrot)$, which includes zero-point energy and thermal contributions to the gas-phase vibrational−rotational energy.

The 298 K enthalpy of activation $H_{298}^\ddagger$ and the 298 K free energy of activation are evaluated by conventional transition state theory as[19]

$$\Delta H_{298}^\ddagger = H_{298}^\ddagger - H_{298}^R \quad (5)$$

and

$$\Delta G_{298}^\ddagger = G_{298}^\ddagger - G_{298}^R \quad (6)$$

where ‡ denotes the transition state (assumed here to be located at the saddle point), and R denotes the reactant. Kinetic isotope effects were calculated by conventional transition state theory[19,20] with a unit transmission coefficient with the ISOEFF98[21] program.

In all cases with discrete water molecules, we examined all reasonable locations for attaching a water molecule and all reasonable conformations, and we selected the lowest-energy one in the gas phase. For the mixed discrete + continuum calculations, we reoptimized these favored structures in the presence of continuum solvent. All optimized **Z** structures have no imaginary frequencies. All optimized **T** structures have one imaginary frequency corresponding to the reaction coordinate.

Atomic partial charges were calculated with the CM2 charge model[22] using MN-GSM.[14]

As stated above, the continuum liquid for the continuum and mixed calculations is modeled by the SM5.42/HF/6-31G(d) method. These calculations were carried out with the MN-GSM module[14] of GAUSSIAN 98.[15] The MC-QCISD calculations were carried out by using the MULTILEVEL[16] program.
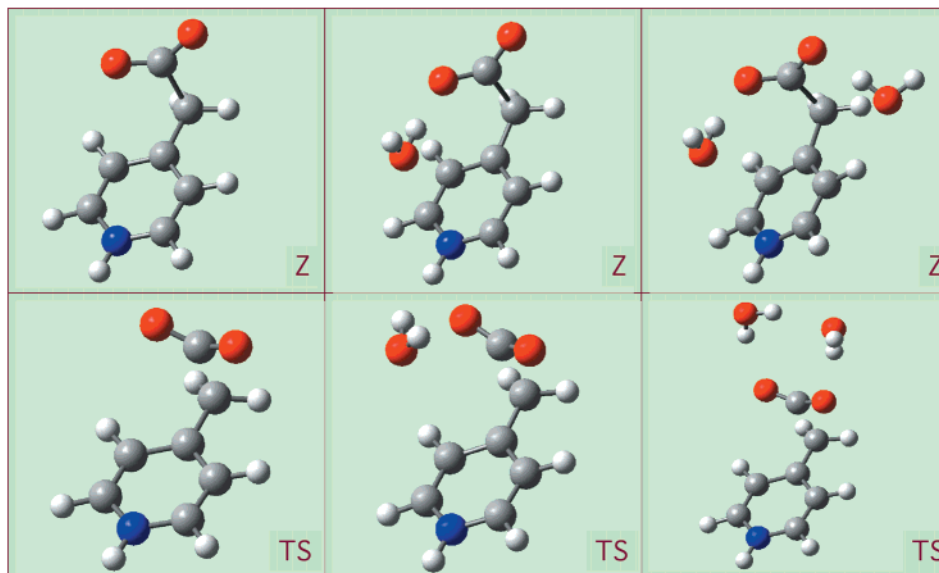
Figure 1. Optimized structures for zwitterion (left side) and transition state (right side) without continuum solvent. The top, middle, and bottom rows correspond to 0, 1, and 2 waters, respectively. Note that the benzyl−carboxyl carbon−carbon bond length r is denoted by a stick when it is less than 1.61 Å but not when it is larger than this.
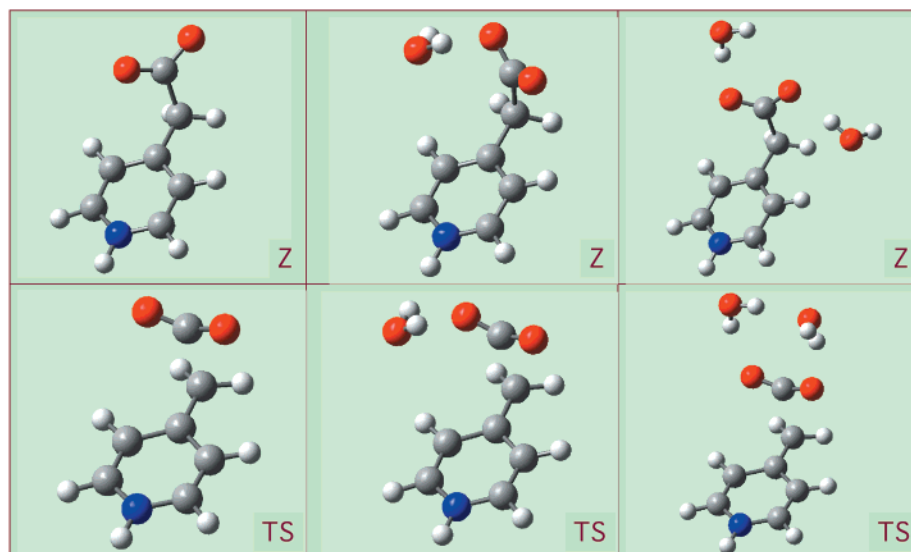

Figure 2. Same as Figure 1 but in the presence of continuum solvent.

We also repeated the calculations using the C-PCM-UAHF model[17] of Gaussian 98. Again we corrected the gas-phase result with MC-QCISD (in this case evaluated by a gas-phase calculation at the C-PCM-UAHF liquid-phase geometry), and again we used the 6-31G* basis for the liquid-phase calculations. This model includes electrostatic terms calculated by the COSMO[18] model for a continuum dielectric representation of the solvent. It also includes cavitation, dispersion, and repulsion. Whereas the GB calculations use a superposition of atomic spheres to define the explicit-system cavity, the C-PCM-UAHF model uses united atoms. Another significant difference is that SM5.42 is based on class IV atomic partial charges, whereas the COSMO algorithm involves the actual solute density $\psi_1 * \psi_1$. Furthermore, the SM5.42 model includes explicit solvent-structure terms that account (in principle) for the deviation of first-solvation-shell hydrogen bonding interactions from bulk electrostatics, but the C-PCM-UAHF model does not.

SCHEME 1
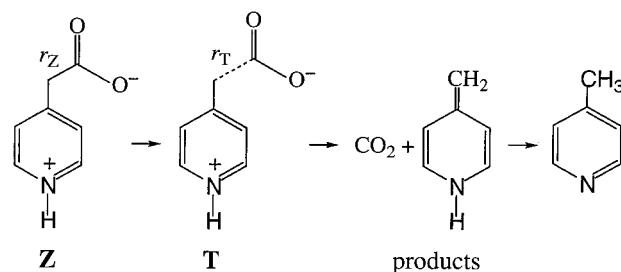
3. Results

The reaction is shown in Scheme 1, where **Z** denotes the zwitterion and **T** the transition state. Figures 1 and 2 give the optimized structures. Table 1 gives the values r_Z and r_T of the breaking C−C bond in the optimized **Z** and **T** structures. Table 1 also gives $\Delta H_0^{\ddagger}$ and $\Delta G_{298}^{\ddagger}$ calculated in the manner de-

TABLE 1: Geometries, Activation Parameters, and Kinetic Isotope Effects[a]

label	description	r_Z	r_T	$\Delta H^{\ddagger}_{298}$	$\Delta G^{\ddagger}_{298}$	k_{12}/k_{13}	k_{16}/k_{18}	k_{14}/k_{15}
0D	gas-phase	1.64	1.79	−4.6	−4.7	1.035	0.999	1.003
1D	discrete (1)[b]	1.60	1.96	−1.7	−2.1	1.048	0.996	1.007
2D	discrete (2)	1.59	1.97	5.5	1.1	1.052	0.995	1.007
0C	SM5.42	1.54	2.23		24.2	1.057	0.989	1.009
1C	discrete(1) + SM5.42	1.54	2.19		21.2	1.058	0.990	1.008
2C	discrete(2) + SM5.42	1.54	2.21		18.3	1.058	0.992	1.009
0C	C-PCM-UAHF[c]	1.54	2.14		18.5	1.064	0.992	1.008
	experiment (extrap)[d]					1.052[e]	0.990[f]	1.007[g]
	experiment (75:25)[h]					1.056[e]	0.995[f]	1.002[g]

[a] Distances are in angstroms, and free energy and enthalpy are in kcal/mol; all KIEs are for 298 K. [b] The numbers in parentheses are the number of discrete solvent molecules. [c] Continuum COSMO model (based on UAHF cavity, as implemented in Gaussian 98). [d] Extrapolated to 100% water from 75% water/25% dioxane and 50% water/50% dioxane. [e] Reference 23. [f] Reference 24. [g] Reference 25. [h] Experimental value for 75% water/ 25% dioxane.

TABLE 2: Selected Additional Properties of Zwitterion and Transition State[a]

	zwitterion		transition state						
label	r_{CO}	θ_{OCO}	r_{CO}	θ_{OCO}	q_{C-1}	q_{C-2}	q_{O-1}	q_N	q_{H_N}	$\omega^{\ddagger}$
0D	1.21	135	1.20	141	0.36	−0.29	−0.44	−0.34	0.33	$397i[-7i]^b$
1D	1.22	132	1.19	144	0.40	−0.33	−0.40	−0.35	0.33	$556i[-11i]$
2D	1.23	131	1.18	146	0.41	−0.33	−0.38	−0.36	0.33	$557i[-11i]$
0C	1.24	128	1.17	151	0.44	−0.39	−0.37	−0.34	0.35	$737i[-17i]$
1C	1.24	128	1.16	152	0.45	−0.39	−0.36	−0.35	0.35	$718i[-16i]$
2C	1.24	127	1.16	153	0.41	−0.33	−0.34	−0.35	0.35	$688i[-15i]$

[a] Bond distances are in angstroms, bond angles are in degrees, atomic partial charges are in units of electron charge, and imaginary frequencies along the reaction coordinates are in cm^{-1}. When q_{O-1} and q_{O-2} differ or when the two r_{CO} values differ, we give the average. [b] Values in brackets are the frequency shift upon ^{13}C substitution.

scribed above. Note that in all cases we give the activation parameters for **Z** as reactant even though in the absence of solvent the nonzwitterionic form of the reactant has a lower energy. The final two columns of Table 1 give transition-state-theory calculations of kinetic isotope effects (KIEs) for substitution of ^{13}C in the carboxyl carbon (C-1), for substitution of ^{18}O in one of the carboxyl oxygens (O-1 and O-2), and for substitution of ^{15}N in the ring. Note that the experiment corresponds to only one oxygen being labeled. For ^{18}O, values reported are averages for both possible positions. Again the reactant is taken as **Z** for all calculations because the goal is to model bulk aqueous solution where the reactant is definitely **Z**. In all cases, the KIE is listed as the ratio of the rate constant for the unsubstituted case to that for heavy-atom isotopic substitution.

We note that the MC-QCISD gas-phase correction to ΔH_{298} and ΔG_{298} (which is already included in Table 1) amounts to −2.6 kcal/mol at the SM5.42 geometries but −3.1 kcal/mol at the C−PCM-UAHF geometries.

The last two rows give experimental[23–25] KIEs at 298 K for comparison. The KIEs were measured in dioxane/water solution containing up to 75% water. Because known properties of dioxane/water mixtures change nonlinearly with composition and properties of the mixture containing 75% water are close to those for pure water, one might expect KIEs to behave similarly; thus, we list the final experimental value as the value for 75% water. For comparison, though, we also list a value for 100% water that is obtained by linear extrapolation. We might expect the actual experimental result to lie between these two values with a further ± 0.001 to account for the standard deviation of the experiments.

Table 2 lists some additional properties of the zwitterion and transition state. First it gives the C−O distance and O−C−O bond angles in the carboxyl moiety (the two C−O distances are not identical by symmetry but are usually the same to the precision tabulated; when they are not, we give the average).

Table 2 gives atomic partial charges at the transition state for the carboxyl C, the methylene C (labeled C-2), one of the carboxyl oxygens (those for the other are usually the same to the precision tabulated, but when the two charges differ we give the average), the nitrogen, and the hydrogen on the N. It also gives the imaginary frequency for the isotopically unsubstituted case and its shift upon ^{13}C substitution.

4. Discussion

Because of the lack of conformational averaging in the mixed discrete-continuum models (i.e., one should but does not sum over all possible conformations of the discrete solvent molecules) and the lack of explicit hydrogen bonding terms in the C-PCM-UAHF calculations, we believe that the full SM5.42 continuum results (labeled 0C in Table 1) are the most reliable estimates of the true situation in aqueous solution, although it is somewhat disconcerting that adding one or two explicit water molecules to the full continuum result has such a large effect. The KIEs in Table 1 do not allow one to judge on the basis of experiment whether the SM5.42 model or the discrete(n) + SM5.42 model is a better representation of the true situation in aqueous solution. Although we did not perform a complete search to identify the lowest-energy structure with three explicit water molecules, we did enough calculations with three waters to be sure that such an approach would not resolve this issue. We conclude that, in the absence of experimental absolute reaction rates in water, we cannot provide a definitive answer to the second question raised in the Introduction.

We turn next to the first question: how well does microsolvation in a cluster, as exemplified by rows 1D and 2D in the tables, mimic bulk solvation, as exemplified by rows 0C, 1C, and/or 2C. The answer is resoundingly clear: not well at all. The free energy of activation is greatly underestimated, and the C(1)−C(2) bond length is greatly overestimated in the zwitterion and even more greatly underestimated at the transition state.

Table 2 shows that the atomic partial charges do not show large differences among the various calculations, except for the charges on the carboxyl carbon and methylene carbon (which are the atoms involved in $C(1)-C(2)$ bond); these charges vary as much as 0.05 and 0.06, respectively, in the models that include solvent.

In previous work, Zipse et al.[26] modeled the decarboxylation of benzisoxisole-3-carboxylic with two discrete water molecules, and Bach and Canepa[27] studied the aqueous decarboxylation of aminoformylacetic acid with a supermolecule approach involving six water molecules. These investigators did not employ continuum solvation, but one might expect differences between discrete and continuum models for those substrates that are similar to the large differences found here. It would be interesting to reinvestigate those systems.

One might argue that the discrete model fails because it includes only one or two solvent molecules. However, that is the point of the paper, to test quantitatively how well a small cluster models bulk solvation. Furthermore, there is a very significant difficulty with using larger numbers of solvent molecules in a discrete solvation model, namely, conformational averaging. As one adds more solvent molecules, the number of solvent conformations rapidly becomes unmanageable, and a proper conformational average over these conformations requires a full explicit-solvent liquid simulation. The goal of the present paper was to test quantitatively how well one can use optimized small clusters to predict or model liquid-phase free energies of activation for a process creating charge separation, not to test full explicit-solvent liquid simulations.

5. Concluding Remarks

Discrete, continuum, and mixed discrete-continuum models give quite different free energies of activation for decarboxylation of 4-pyridylacetic acid zwitterion in water, with values in the ranges of $(-2)-1$, 18.5−24, and 18.3−21 kcal/mol, respectively, as compared to a gas-phase value of −5 kcal/mol (with all values at 298 K). It is not clear which of these models is most realistic. The SM5.42 continuum model used here does include explicit terms incorporating first-solvation-shell effects, but it is possible that these terms, which were parametrized primarily against data for uncharged species, misestimate the first-solvation shell effects for zwitterions. On the other hand, the cluster model may be inadequate to represent bulk solvation for several possible reasons: (i) the solvent-shell conformations may differ in the cluster and the bulk, (ii) the properties of the solvent molecules (e.g., their dipole moments and polarizabilities) may differ in the cluster and the bulk, (iii) the error in the electronic structure calculations of the strength of solute−solvent interactions is difficult to gauge for transition states of large molecules, and (iv) the cluster model lacks long-range solvent polarization effects, extending beyond the first solvation shell.

Although the availability of three different kinetic isotope effects for the present problem makes it an excellent test case for comparing theory to experiment, the actual comparisons of theory to experiment presented in this paper do not definitively indicate which of the discrete, continuum, and mixed discrete−continuum models is most accurate. They do, however, show that a measurement of (or more definitive calculation of) the absolute reaction rate (to yield the phenomenological free energy of activation) would be very useful in testing the calculations. The present calculations by themselves do not clarify whether the difference between the continuum and mixed discrete−continuum models should be considered as a deficiency of the former, of the latter, or of both.

References and Notes

(1) (a) Meot-Nir, M. *Mol. Struct. Energy* **1987**, *4*, 71. (b) Farrar, J. M. In *Cluster Ions*; Ng, C.-Y., Baer, T., Powis, I., Eds.; Wiley: Chichester, 1993; p 243. (c) Syage, J. A. *Understanding Chem. React.* **1994**, *7*, 289. (d) Papanikolas, J. M.; Campagnola, P. J.; Vorsa, V.; Nadal, M. E.; Buchenau, H. K.; Parson, R.; Lineberger, W. C. *Adv. Ser. Phys. Chem.* **1995**, *6*, 616. (e) Knochenmuss, R. *J. Chim. Phys.* **1995**, *92*, 445. (f) *Chemical Reactions in Clusters*; Bernstein, E. R., Ed.; Oxford University Press: New York, 1996. (g) Coe, J. V. *J. Phys. Chem.* **1997**, *101*, 2055. (h) Kebarle, P.; Searles, S. K.; Zolla, A.; Scarborough, J.; Arshadi, M. *J. Mass Spectrom.* **1997**, *32*, 915. (i) Castleman, A. W., Jr. *Adv. Gas-Phase Ion Chem.* **1998**, *3*, 185. (j) Uggerud, E. *Int. J. Mass Spectrom.* **1999**, *182/183*, 13. (k) Kebarle, P. *Int. J. Mass Spectrom.* **2000**, *200*, 313. (l) Zhong, Q.; Castleman, A. W., Jr. *Chem. Rev.* **2000**, *100*, 4039.

(2) Cramer, C. J.; Truhlar, D. G. *Chem. Rev.* **1999**, *99*, 2161.

(3) (a) Sanchez Marcos, E.; Pappalardo, R. R.; Rinaldi, D. *J. Phys. Chem.* **1991**, *95*, 8928. (b) Zeng, J.; Craw, J. S.; Hush, N. S.; Reimers, J. R. *Chem. Phys. Lett.* **1993**, *206*, 323. (c) Sanchez Marcos, E.; Terryn, B.; Rivail, J.-L. *J. Phys. Chem.* **1985**, *89*, 4695. (d) Tuñón, I.; Rinaldi, D.; Ruiz-Lopez, M. F.; Rivail, J. L. *J. Phys. Chem.* **1995**, *99*, 3798. (e) Alemán, C.; Galembeck, S. E. *Chem. Phys.* **1998**, *232*, 151. (f) Bräuer, M.; Mosquera, M.; Pérez-Lustres, J. L.; Rodríguez-Prieto, F. *J. Phys. Chem. A* **1998**, *102*, 10736. (g) Martínez, J. M.; Pappalardo, R. R.; Sanchez Marcos, E. *J. Phys. Chem. A* **1997**, *101*, 4444.

(4) Leach, A. R. *Molecular Modeling*, 2nd ed.; Prentice Hall: New York, 2001.

(5) *Combined Quantum Mechanical and Molecular Mechanical Methods*; Gao, J., Thompson, M. A., Eds.; American Chemical Society: Washington, DC, 1998.

(6) Halgren, T. A. *Curr. Opin. Struct. Biol.* **2001**, *11*, 236.

(7) Sicinska, D.; Truhlar, D. G.; Paneth, P. *J. Am. Chem. Soc.* **2001**, *123*, 7863.

(8) Roothaan, C. C. J. *Rev. Mod. Phys.* **1951**, *23*, 69.

(9) Radom, L.; Hariharan, P. C.; Pople, J. A.; Schleyer, P. v. R. *J. Am. Chem. Soc.* **1974**, *96*, 599.

(10) (a) Zhu, T.; Li, J.; Hawkins, G. D.; Cramer, C. J.; Truhlar, D. G. *J. Chem. Phys.* **1998**, *109*, 9117. (b) Li, J.; Hawkins, G. D.; Cramer, C. J.; Truhlar, D. G. *Chem. Phys. Lett.* **1998**, *288*, 293. (c) Li, J.; Zhu, T.; Hawkins, G. D.; Winget, P.; Liotard, D. A.; Cramer, C. J.; Truhlar, D. G. *Theor. Chem. Acc.* **1999**, *103*, 9. (d) Zhu, T.; Li, J.; Liotard, D. A.; Cramer, C. J.; Truhlar, D. G. *J. Chem. Phys.* **1999**, *110*, 5503. (e) Chuang, Y.-Y.; Radhakrishnan, M. L.; Fast, P. L.; Cramer, C. J.; Truhlar, D. G. *J. Phys. Chem. A* **1999**, *103*, 4893.

(11) (a) Hoijtink, G. J.; de Boer, E.; van der Meij, P. H.; Weiland, W. P. *Recl. Trav. Pays-Bas* **1956**, *75*, 487. (b) Peradejordi, F. *Cahiers Phys.* **1963**, *17*, 393. (c) Jano, I. *Compt. Rend. Acad. Sci. Paris* **1965**, *261*, 103. (d) Tapia, O. In *Quantum Theoretical Chemical Reactions*; Daudel, R., Pullman, A., Salem, L., Viellard, A., Eds.; Reidel: Dordrecht, The Netherlands, 1980; Vol. 2, p 25. (e) Tucker, S. C.; Truhlar, D. G. *Chem. Phys. Lett.* **1989**, *157*, 164. (f) Still, W. C.; Tempczyk, A.; Hawley, R. C.; Hendrickson, T. *J. Am. Chem. Soc.* **1990**, *112*, 6127. (g) Cramer, C. J.; Truhlar, D. G. *J. Am. Chem. Soc.* **1991**, *113*, 8305, 9901E.

(12) (a) Lee, B.; Richards, F. M. *J. Mol. Biol.* **1971**, *55*, 379. (b) Hermann, R. B. *J. Phys. Chem.* **1972**, *76*, 2754.

(13) Fast, P. L.; Truhlar, D. G. *J. Phys. Chem. A* **2000**, *104*, 6111.

(14) Xidos, J. D.; Li, J.; Hawkins, G. D.; Winget, P. D.; Zhu, T.; Rinaldi, D.; Liotard, D. A.; Cramer, C. J.; Truhlar, D. G.; Frisch, M. J. MN-GSM, version 99.7; University of Minnesota: Minneapolis, MN, 2001.

(15) Frisch, M. J.; Trucks, G. W.; Schlegel, H. B.; Scuseria, G. E.; Robb, M. A.; Cheeseman, J. R.; Zakrzewski, V. G.; Montgomery, J. A., Jr.; Stratmann, R. E.; Burant, J. C.; Dapprich, S.; Millam, J. M.; Daniels, A. D.; Kudin, K. N.; Strain, M. C.; Farkas, O.; Tomasi, J.; Barone, V.; Cossi, M.; Cammi, R.; Mennucci, B.; Pomelli, C.; Adamo, C.; Clifford, S.; Ochterski, J.; Petersson, G. A.; Ayala, P. Y.; Cui, Q.; Morokuma, K.; Malick, D. K.; Rabuck, A. D.; Raghavachari, K.; Foresman, J. B.; Cioslowski, J.; Ortiz, J. V.; Stefanov, B. B.; Liu, G.; Liashenko, A.; Piskorz, P.; Komaromi, I.; Gomperts, R.; Martin, R. L.; Fox, D. J.; Keith, T.; Al-Laham, M. A.; Peng, C. Y.; Nanayakkara, A.; Gonzalez, C.; Challacombe, M.; Gill, P. M. W.; Johnson, B. G.; Chen, W.; Wong, M. W.; Andres, J. L.; Head-Gordon, M.; Replogle, E. S.; Pople, J. A. *Gaussian 98*; Gaussian, Inc.: Pittsburgh, PA, 1998.

(16) Rodgers, J. M.; Lynch, B. J.; Fast, P. L.; Chuang, Y.-Y.; Pu, J.; Truhlar, D. G. multilevel, version 2.2; University of Minnesota: Minneapolis, MN, 2001.

(17) Barone, V.; Cossi, M. *J. Phys. Chem. A* **1998**, *102*, 1995. (b) Barone, V.; Cossi, M.; Tomasi, J. *J. Chem. Phys.* **1997**, *107*, 3210.

(18) Klamt, A.; Schuürmann, G. *J. Chem. Soc., Perkin Trans. 2* **1993**, *1993*, 799.

(19) Kreevoy, M. M.; Truhlar, D. G. In *Investigation of Rates and Mechanism of Reactions*, 4th ed.; Bernasconi, C. F.; Ed.; Techniques of Chemistry, Vol. VI, Part 1; Wiley & Sons: New York, 1985; p 13.

(20) Bigeleisen, J. *J. Chem. Phys*. **1949**, *17*, 675.

(21) Anisimov, V.; Paneth, P. *J. Math. Chem*. **1999**, *26*, 75.

(22) Li, J.; Zhu, T.; Cramer, C. J.; Truhlar, D. G. *J. Phys. Chem. A* **1998**, *102*, 1820.

(23) Marlier, J. F.; O'Leary, M. H. *J. Am. Chem. Soc*. **1986**, *108*, 4896.

(24) Headley, G. W.; O'Leary, M. H. *J. Am. Chem. Soc*. **1990**, *112*, 1984.

(25) Sicinska, D.; Lewandowicz, A.; Vokal, S.; Paneth, P. *J. Org. Chem*. **2001**, *66*, 5534.

(26) Zipse, H.; Apaydin, G.; Houk, K. N. *J. Am. Chem. Soc*. **1995**, *117*, 8608.

(27) Bach, R. D.; Canepa, C. *J. Am. Chem. Soc*. **1997**, *119*, 11725.